Auger width and branching ratios for berylliumlike $1s2s^2np\,^1P^o$ and $1s2p^3\,^1P^o$ resonances and photoionization of beryllium from $1s^22s^2\,^1S$

Hsin Lin,[1] Chen-Shiung Hsue,[2] and Kwong T. Chung[1]
[1]*Department of Physics, North Carolina State University, Raleigh, North Carolina 27695–8202*
[2]*Department of Physics, National Tsing-Hua University, Hsin-Chu 300, Taiwan, Republic of China*
(Received 19 September 2001; published 12 February 2002)

The photoionization cross section (PICS) of Be from the ground state is studied with the saddle-point complex-rotation method for photon energies from 25 to 122 eV. A full-core plus correlation wave function is used for the ground state. For the resonances in the continuum, the energy and width for the singly core-excited Be-like $1s2s^22p\,^1P^o$, $1s2p^3\,^1P^o$, and $1s2s^23p\,^1P^o$ are calculated to high precision. The PICS are studied with a single open-channel approximation as well as fully coupled open channels. The Auger decay branching ratios of these states are studied to check the spin-alignment theory recently proposed by Chung. These results are compared with the existing theoretical and experimental data in the literature. For beryllium, our energy and width of $1s2s^22p$ are 115.513 eV and 36.6 meV and those of $1s2s^23p$ are 121.420 eV and 50.4 meV, which agree with the experiment of Caldwell *et al.*, [Phys. Rev. A **51**, 542 (1990)].

DOI: 10.1103/PhysRevA.65.032706 PACS number(s): 32.80.Fb, 32.80.Hd, 32.70.Fw, 31.15.Ar

I. INTRODUCTION

In 1990, Caldwell *et al.* [1] reported an experimental study of Be $1s^22s^2$ under synchrotron radiation. They found that the most prominent decay channel for the $1s2s^22p\,^1P^o$ is the $1s^22p$ channel rather than the expected $1s^22s$ channel. This paper has stimulated considerable interest. In this work, we carry out a calculation on the photoionization cross section for Be using a saddle-point complex-rotation method [2]. The photoabsorption experiment is strongly symmetry selective. For photon energies from 25 to 122 eV, there are only two core-excited $^1P^o$ resonances ($1s2s^2np\,^1P^o$) affecting the cross section, namely

$$1s^22s^2+h\nu\rightarrow\begin{cases}1s2s^22p\,^1P, & \Delta E_{1s\rightarrow 2p}=115.5\ \text{eV}\\ 1s2s^23p\,^1P, & \Delta E_{1s\rightarrow 3p}=121.4\ \text{eV}.\end{cases}$$

These resonance states decay by electron emission. Caldwell *et al.* found that the decay to the ground-state ($1s^22s$) channel is almost invisible. That is,

$$1s2s^22p\,^1P^o\rightarrow\begin{cases}1s^22s+e & \text{less than } 2\%\\ 1s^22p+e & \text{more than } 95\%.\end{cases}$$

This feature for Be may occur in slow ion-surface collision experiment [3]. The lack of ground-state channel appears to be a common feature for the Be-like series [4]. For this $1s2s^22p\,^1P^o$, it mainly decays via one channel ($1s^22p+e$). But, for $1s2s^23p\,^1P^o$ and $1s2s^24p\,^1P^o$, there are two or more important decay channels. In these Auger decays, the outer electron can be considered as a spectator. In some theoretical studies, the importance of the spectator in Auger decay has been taken into consideration, for example, in calculating the photoexcited $1s^{-1}np$ for Ne [5] and the photodetachment on Li^- [6]. For beryllium $1s2s^23p$, we have [1]

$$1s2s^23p\,^1P^o\rightarrow\begin{cases}1s^23p+e, & 78\%\\ 1s^24p+e, & 22\%.\end{cases}$$

Recently, Jiménez-Mier *et al.* [7] carried out a high-resolution experiment on Be. In this experiment, the decay mode for $1s2s^2np\,^1P^o(n=2,3)$ found previously by Caldwell *et al.* is reconfirmed. In addition, they also studied the decay modes of higher resonances for n up to 6. On the theoretical side, they have made a "shake" calculation in terms of the projection of the bound electron wave function to compare with experimental data.

To explain the Auger branching ratios for multiply excited atomic systems, a spin-alignment-dependent theory was proposed by Chung [8]. It gives the physical reason behind the relative magnitude of the partial widths. Many examples of three-electron systems have been calculated to support this theory. Our study is intended to investigate the validity of this theory for four-electron systems and to compare our results with experiments.

The resonances studied in this work are inner-shell core-excited states which lie highly above the ionization threshold. To determine the closed-channel part of the wave function, a saddle-point method [9] is used. A $1s$-vacancy orbital is explicitly built into the wave function to remove the continuum. The energy and the wave function for the resonance are obtained through a minimax procedure. Accurate results for 2–4 electron atoms have been achieved by this method in the past [10–16].

To include the contribution from the open channels, we use the saddle-point complex-rotation method [17]. Square integrable wave functions are used to calculate the resonance width. We first include one open channel at a time for an approximate partial width and the total width is calculated by including all important open channels. For all the resonances investigated in this work, the sum of the partial widths deviates from the total width by 1% or 2%. Finally, the photo-

ionization cross section (PICS) is computed using a method similar to Chung [2,18] following a suggestion by Rescigno and McKoy [19].

The energy and Auger width for Be $1s2s^2np(n=2-6)$ $^1P^o$ are calculated in this work. When we extend the calculation from B to Ne, the three lowest $^1P^o$ states, $1s2s^22p$, $1s2p^3$, and $1s2s^23p$ are investigated. The theories for our calculation are reviewed in Sec. II. The calculated results are presented and compared with experimental data and other theoretical results in Sec. III. The discussion of the Auger decay modes is also given in this section. Section IV is short conclusions.

II. THEORY

A. The variation principal and the saddle-point method

The zeroth-order nonrelativistic Hamiltonian for a four-electron system is (in a.u.)

$$H_0=\sum_{i=1}^{4}\left(-\frac{1}{2}\nabla_i^2-\frac{Z}{r_i}\right)+\sum_{\substack{i,j=1\\ i<j}}^{4}\frac{1}{r_{ij}}. \tag{1}$$

To calculate $^1P^o$ resonances, a multiconfiguration interaction (MCI) wave function in LS coupling scheme is used. The basis functions are eigenfunctions of L^2, S^2, L_z, and S_z. Here L and S are the total orbital and spin angular momentum of the system. The basis functions may be written as

$$\Phi_{n(i),l(i)}(\vec{r}_1,\vec{r}_2,\vec{r}_3,\vec{r}_4)=\varphi_{n(i)}(R)Y_{l(i)}^{LL_z}(\hat{R})\chi_{SS_z}. \tag{2}$$

The radial function is the product of the Slater orbitals

$$\varphi_{n(i)}(R)=\prod_{j=1}^{4}r_j^{n_j}e^{-\alpha_j r_j}. \tag{3}$$

The orbital angular part is given by

$$Y_{l(i)}^{LL_z}(\hat{R})=\sum_{m_j}\langle l_1m_1l_2m_2|l_{12}m_{12}\rangle\langle l_{12}m_{12}l_3m_3|l_{123}m_{123}\rangle \times\langle l_{123}m_{123}l_4m_4|LL_z\rangle\prod_{j=1}^{4}Y_{l_jm_j}(\Omega_j), \tag{4}$$

where $l(i)=[(l_1,l_2)l_{12},l_3]l_{123},l_4$. This implies that the angular momenta of electrons 1 and 2 couple into l_{12}, which in turn couples with l_3 into l_{123}. The final P state is obtained by coupling l_{123} with l_4. Similarly, the spin angular part is given by

$$\chi_{SS_z}=[(S_1,S_2)S_{12},S_3]S_{123},S_4. \tag{5}$$

For a singlet, two spinor functions are possible,

$$\chi^1=\left[\left(\frac{1}{2},\frac{1}{2}\right)1,\frac{1}{2}\right]\frac{1}{2},\frac{1}{2}, \tag{6}$$

$$\chi^2=\left[\left(\frac{1}{2},\frac{1}{2}\right)0,\frac{1}{2}\right]\frac{1}{2},\frac{1}{2}. \tag{7}$$

For a singly core-excited state, only one electron is allowed to occupy the $1s$ orbital and a $1s$ vacancy needs to be built into the closed-channel wave function Ψ_c

$$\Psi_c=A\sum_{n(i),l(i)}C_{n(i)}^{l(i)}(1-Q_j)\Phi_{n(i),l(i)}(\vec{r}_1,\vec{r}_2,\vec{r}_3,\vec{r}_4). \tag{8}$$

A is an antisymmetrization operator. C's are linear coefficients and $Q_j=|\varphi_{1s}(\vec{r}_j)\rangle\langle\varphi_{1s}(\vec{r}_j)|$ is the projection operator for the vacancy where

$$\varphi_{1s}(\vec{r}_j)=2q^{3/2}e^{-qr_j}. \tag{9}$$

The parameter q can be interpreted as the effective nuclear charge seen by the $1s$-vacancy orbital. A secular equation is constructed from

$$\delta\langle H_0\rangle=\delta\frac{\langle\Psi_c|H_0|\Psi_c\rangle}{\langle\Psi_c|\Psi_c\rangle}=0. \tag{10}$$

It is solved to determine the C's and the eigenenergy E_c, which is a function of two classes of nonlinear parameters, $E_c=E_c(\alpha,q)$. The resonance energy is given by a minimum of α_s and a maximum of q.

B. The restricted-variation method

Adding more terms in a secular equation to saturate the functional space can, in principle, give a more accurate energy. For nonorthogonal basis, such as Slater orbitals, however, this may cause numerical instability due to linear dependence. The restricted-variation method [20] allows us to saturate the functional space and avoids numerical instability by treating the wave function Ψ_c as a single term. A more accurate wave function Ψ is constructed as

$$\Psi=d_0\Psi_c+\sum_i d_i\Phi_i. \tag{11}$$

The d's are linear coefficients and are determined by solving a new secular equation. The improved energy $\Delta E_{RV}=E_c(\text{new})-E_c(\text{old})$ can be calculated. Although the basis functions Φ_i's are similar to those of Ψ_c, as long as Φ_i is independent of one of the basis functions in Ψ_c, numerical instability is avoided. Each of the nonlinear parameters α's in Φ_i is optimized and the number of terms can be increased significantly to achieve a higher accuracy.

C. The perturbation correction

The relativistic and mass polarization corrections are obtained with first-order perturbation theory using the perturbation Hamiltonian H'

$$\Delta E_{rel}=\langle\Psi_c|H'|\Psi_c\rangle, \tag{12}$$

where $H'=H_1+H_2+H_3+H_4+H_5$ and

(1) $H_1=-(1/8c^2)\Sigma_{i=1}^4\vec{P}_i^4$ (kinetic energy correction)

(2) $H_2=-(Z\pi/2c^2)\Sigma_{i=1}^4\delta(\vec{r}_i)$ (Darwin term)

(3) $H_3=-(\pi/c^2)\sum_{i<j}^{4,j=1}(1+\frac{8}{3}\vec{s}_i\cdot\vec{s}_j)\delta(\vec{r}_{ij})$ (electron-electron contact term)

(4) $H_4=-(1/M)\sum_{i<j}^{4,j=1}\vec{\nabla}_i\cdot\vec{\nabla}_j$ (mass polarization correction)

(5) $H_5=-(1/2c^2)\sum_{i<j}^{4,j=1}(1/r_{ij})(\vec{P}_i\cdot\vec{P}_j+\{[\vec{r}_{ij}(\vec{r}_{ij}\cdot\vec{P}_i)\cdot\vec{P}_j]/r_{ij}^2\})$ (retardation potential).

M is the nuclear mass in a.u. and $c=137.036$ is the velocity of light.

D. The complex-rotation method

The total wave function for the resonance includes both the closed and open channels, i.e.,

$$\Psi(1,2,3,4)=\Psi_c(1,2,3,4)+A\sum_{o,j}\Phi_o(1,2,3)U_{o,j}(4), \tag{13}$$

where Φ_o's are the target states of the open channels and $U_{o,j}$ represents the outgoing electron. The open-channel components in real coordinate space are not square integrable. However, if we assume

$$U_{o,j}=\sum_n d_{o,j,n}r^n e^{-\alpha_j r} \tag{14}$$

and make an inverse complex scaling $r\rightarrow re^{-i\theta}$ in U, the complex resonance energy of the resonance can be calculated with a variation method. Proper angular and spin coupling between Φ_o and $U_{o,j}$ is implicitly assumed in Eq. (13). For narrow resonance, the coupling between the closed and open channels is weak. The resonance wave function can be approximated by the closed-channel wave function. In computation, the nonlinear parameters α's in Ψ_c obtained from the saddle-point calculation are fixed, but the linear coefficients C's in Ψ_c and the d's are recalculated to allow for full interaction between the closed and open channels. The real part of the eigenvalue gives us the resonance energy E_{res} and the imaginary part gives us the width of the resonance. $\Delta E_{shift}=E_{res}-E_c$ represents the energy shift due to the interaction. In this work, the target states considered are $1s^22s$ and $1s^2np(n=2-7)$.

Finally, we obtain the energy of the resonance

$$E_{total}=E_c+\Delta E_{RV}+\Delta E_{rel}+\Delta E_{shift}. \tag{15}$$

E. Photoionization cross section

The PICS is obtained from the imaginary part of the polarization. This method is suggested by Rescigno and McKoy [19]. Highly accurate results for lithium have been achieved with this method [2,18]. The PICS may be written as

$$\sigma(\omega)=\frac{4\pi^2}{3c}\omega\sum_{E_f=Eo+\omega}|\langle\Psi_o|\vec{D}|\Psi_f\rangle|^2, \tag{16}$$

where ω is the photon energy, $\vec{D}$ is the dipole length operator, Ψ_o is the initial ground-state wave function and Ψ_f is the final-state wave function.

The polarizability of an atomic system is given by

$$\alpha(\omega)=\left(\sum_n\frac{|\langle\Psi_o|\vec{D}|\Psi_n\rangle|^2}{E_n-E_o-\omega}+\int\frac{|\langle\Psi_o|\vec{D}|\Psi_E\rangle|^2}{E-E_o-\omega-i\epsilon}dE+\sum_n\frac{|\langle\Psi_o|\vec{D}|\Psi_n\rangle|^2}{E_n-E_o+\omega}\right)\Big/3. \tag{17}$$

Defining

$$\alpha_-(\omega)=\left(\sum_n\frac{|\langle\Psi_o|\vec{D}|\Psi_n\rangle|^2}{E_n-E_o-\omega}+\int\frac{|\langle\Psi_o|\vec{D}|\Psi_E\rangle|^2}{E-E_o-\omega-i\epsilon}dE\right)\Big/3, \tag{18}$$

then

$$\mathrm{Im}\,\alpha_-(\omega)=\frac{1}{3}\pi|\langle\Psi_o|\vec{D}|\Psi_f(E=E_o+\omega)\rangle|^2. \tag{19}$$

That is,

$$\sigma(\omega)=\frac{4\pi\omega}{c}\mathrm{Im}\,\alpha_-(\omega). \tag{20}$$

To calculate $\alpha_-(\omega)$, we construct a functional

$$F=\langle\Psi_E|H_o-E_i-\omega|\Psi_E\rangle+\langle\Psi_o|D|\Psi_E\rangle+\langle\Psi_E|D|\Psi_o\rangle. \tag{21}$$

We complex scale Ψ_E and solve Ψ_E by finding the extremum for F. Finally, $\alpha_-(\omega)$ is given by the expression

$$\alpha_-(\omega)=\langle\Psi_E|D|\Psi_o\rangle/3. \tag{22}$$

To obtain high-precision PICS, a full-core plus correlation wave function is used for the $1s^22s^2\,{}^1S$ wave function,

$$\Psi_o(1,2,3,4)=A\left(\sum_{i=1}^{49}\Psi_{1s^2}(1,2)c_i\Phi_i(3,4)+\sum_{j=1}^{801}d_j\Phi_j(1,2,3,4)\right). \tag{23}$$

Ψ_{1s^2} is a 159-term core wave function. $\Phi_i(3,4)$'s are the Slater orbitals for the two $2s$ electrons. $\Phi_j(1,2,3,4)$'s are CI wave functions to account for intershell correlation. Compared to the usual CI method, Ψ_o is equivalent to a 8592-term wave function.

III. RESULT AND DISCUSSION

A. Energy contribution

The energy E_c for the berylliumlike $^1P^o$ states is calculated with the saddle-point method. It is the energy obtained from the closed-channel wave function. Basis functions of 387–731 terms are used in these calculations. To ensure suf-

TABLE I. Energies for the singlet berylliumlike systems. q is the nonlinear parameter of the $1s$ vacancy. The E_c is the energy calculated by the saddle-point method, ΔE_{RV} represents the energy improvement using the restricted-variation method, ΔE_{rel} is the perturbation corrections, and ΔE_{shift} is the energy shift due to the interaction with open channel (in a.u.). Γ is the total width in meV.

$^1P^o$ state	q	E_c	ΔE_{RV}	ΔE_{rel}	ΔE_{shift}	E_{total}	Γ
^{9}Be $1s2s^22p$	3.410	−10.421 802	−0.000 814	−0.002 053	0.000 275	−10.424 394	37
^{9}Be $1s2s^23p$	3.470	−10.204 670	−0.000 637	−0.002 079	0.000 072	−10.207 314	50
^{9}Be $1s2s^24p$	3.473	−10.163 637	−0.000 571	−0.002 093	0.000 064	−10.166 237	51
^{9}Be $1s2s^25p$	3.473	−10.146 344	−0.001 140	−0.002 086	0.000 041	−10.149 529	52
^{9}Be $1s2s^26p$	3.476	−10.138 155	−0.000 970	−0.002 092	0.000 025	−10.141 192	>48 [a]
^{11}B$^+$ $1s2s^22p$	4.394	−17.201 771	−0.000 977	−0.005 316	0.000 351	−17.207 713	45
^{11}B$^+$ $1s2p^3$	4.453	−16.635 278	−0.001 789	−0.004 620	0.000 435	−16.641 252	27
^{12}C^{2+} $1s2s^22p$	5.384	−25.732 431	−0.001 522	−0.011 517	0.000 390	−25.745 080	53
^{12}C^{2+} $1s2p^3$	5.548	−24.973 280	−0.001 198	−0.009 780	0.000 686	−24.983 572	35
^{12}C^{2+} $1s2s^23p$	5.472	−24.669 262	−0.000 862	−0.010 813	0.000 269	−24.680 668	65
^{14}N^{3+} $1s2s^22p$	6.378	−36.013 832	−0.001 454	−0.022 095	0.000 414	−36.036 967	58
^{14}N^{3+} $1s2p^3$	6.569	−35.063 077	−0.002 175	−0.018 543	0.000 837	−35.082 958	43
^{14}N^{3+} $1s2s^23p$	6.467	−34.320 863	−0.001 245	−0.021 824	0.000 282	−34.344 214	69
^{16}O^{4+} $1s2s^22p$	7.374	−48.045 945	−0.001 162	−0.038 696	0.000 434	−48.085 369	62
^{16}O^{4+} $1s2p^3$	7.604	−46.904 276	−0.001 525	−0.032 354	0.001 186	−46.936 969	50
^{16}O^{4+} $1s2s^23p$	7.474	−45.584 892	−0.001 031	−0.037 992	0.000 365	−45.623 550	72
^{19}F^{5+} $1s2s^22p$	8.371	−61.827 211	−0.001 201	−0.063 298	0.000 452	−61.891 258	65
^{19}F^{5+} $1s2p^3$	8.625	−60.495 039	−0.001 831	−0.052 817	0.001 027	−60.548 660	55
^{19}F^{5+} $1s2s^23p$	8.474	−58.459 624	−0.001 239	−0.061 779	0.000 382	−58.522 260	75
^{20}Ne^{6+} $1s2s^22p$	9.360	−77.358 819	0.000 303	−0.098 217	0.000 341	−77.456 393	68
^{20}Ne^{6+} $1s2p^3$	9.640	−75.836 309	−0.001 767	−0.081 704	0.001 342	−75.918 438	60
^{20}Ne^{6+} $1s2s^23p$	9.474	−72.946 068	−0.008 037	−0.095 515	0.000 464	−73.049 156	78

[a]For Be $1s2s^26p$, the partial width of the $1s^28p$ channel is significant (see Table III), and the $1s^29p$ channel should not be neglected. However, an accurate wave function of this highly excited state is difficult to obtain. Since the $1s^29p$ channel is not included in our calculation, the total width of Be $1s2s^26p$ is expected to be more than 48 meV.

ficient accuracy, the functional space is saturated by a much larger basis set using the restricted-variation method [20]. For each angular component, an additional 400 terms are used in this calculation. The improvement E_{RV} is less than $10^{-4}E_c$ (see Table I), which suggests that the closed-channel energy is well approximated by E_c.

In Table I, we list the energies for all the states calculated in this work. The three lowest $^1P^o$ states of singly core-excited states of Be are $1s2s^2np(n=2-4)$, while those of B to Ne are $1s2s^22p$, $1s2p^3$, and $1s2s^23p$. Be $1s2p^3$ is above the $1s2s^2np$ series. As Z is increased, $1s2p^3$ became lower than $1s2s^23p$.

The value of q, to a certain extent, represents the effective charge seen by the $1s$ vacancy orbital. Because the nuclear charge is half screened by the other $1s$ electron, q is close to $Z-0.5$.

The relativistic and mass polarization corrections are obtained from the first-order perturbation theory. The perturbation corrections ΔE_{rel} increase monotonically from 0.002 a.u. for Be to about 0.098 a.u. for Ne.

ΔE_{shift} is the energy shift due to the interaction between the closed and open channels. For these narrow resonances, ΔE_{shift} is quite small. In our result, ΔE_{shift} of $1s2p^3$ is larger than that of $1s2s^2np$ and they increase monotonically as Z increases.

Based on the results from Table I, we compute the transition energies of the core-excited states from ground states. These energies agree with other theoretical results [21–23] and experimental data as is shown in Table II.

B. Auger width and branching ratios

The Auger decay rate and the lifetime of the core-excited states can be calculated with the complex-rotation method. The complex-rotation calculation with a single open channel gives us an approximate estimate of the partial width for each channel. This partial width should be proportional to the branching ratios of the Augur decay channels in collision experiments. In photoionization experiments, the observed branching ratios are further influenced by the oscillator strengths from the initial state to the different ionization channels. Nevertheless, the Auger partial widths of the resonance state still plays a crucial role in these observed branching ratios. The total width in Table I is obtained by including all important open channels in the complex-rotation calculation. These results are very close to the sum of the partial width for each channel. The maximum difference is less than 2% for the states investigated in this work.

TABLE II. Transition energies from the ground state for the singlet berylliumlike systems.

$^1P^o$ state	This work	Theory	Experiment of Ref. [7]	Experiment of Ref. [1]
^{9}Be $1s2s^22p$	115.513	115.64 [a], 115.66 [b]	115.49±0.04	115.5±0.7
^{9}Be $1s2s^23p$	121.420	121.49 [b]	121.42±0.04	121.4±0.8
^{9}Be $1s2s^24p$	122.537	122.63 [b]	122.52±0.04	
^{9}Be $1s2s^25p$	122.992	123.08 [b]	122.96±0.04	
^{9}Be $1s2s^26p$	123.219		123.16±0.04	
^{11}B$^+$ $1s2s^22p$	194.311			
^{11}B$^+$ $1s2p^3$	209.725			
^{12}C^{2+} $1s2s^22p$	293.58	292.49 [c]		
^{12}C^{2+} $1s2p^3$	314.30			
^{12}C^{2+} $1s2s^23p$	322.543			
^{14}N^{3+} $1s2s^22p$	413.197	412.59 [c]		
^{14}N^{3+} $1s2p^3$	439.156			
^{14}N^{3+} $1s2s^23p$	459.257			
^{16}O^{4+} $1s2s^22p$	553.071	553.15 [c]		
^{16}O^{4+} $1s2p^3$	584.319			
^{16}O^{4+} $1s2s^23p$	620.058			
^{19}F^{5+} $1s2s^22p$	713.167	714.17 [c]		
^{19}F^{5+} $1s2p^3$	749.700			
^{19}F^{5+} $1s2s^23p$	804.840			
^{20}Ne^{6+} $1s2s^22p$	897.025	895.10 [c]		
^{20}Ne^{6+} $1s2p^3$	938.874			
^{20}Ne^{6+} $1s2s^23p$	1016.949			

[a]Theoretical results of Berrington *et al.* [21].
[b]Theoretical results of Voky *et al.* [22].
[c]Theoretical results of Chen [23].

For the decay of $1s2s^22p\ ^1P$, it is observed in the experiments of Caldwell *et al.* [1] that there is a near-100% production of the excited Be^+. This result is consistent with the partial widths obtained in this work (see Tables III–V). To understand the physical reason behind this experimental result, we can make the following arguments according to the spin-alignment theory proposed by Chung [8].

(1) When the orbitals are close together, their electron-electron Coulomb interaction is strong. On the other hand, when two electrons are far away, they have little interaction. Augur decay is most likely to occur when the two electrons are close together.

(2) Pauli exclusion principle suggests that the probability density of two electrons with parallel spin is zero when they are at the same location. This implies that the Auger width caused by the interaction between pairs with parallel spin must be small.

(3) If an Auger decay needs angular momentum exchange or spin flip to occur, it is less likely to happen.

(4) The more the overlap between the wave functions of the initial state and target state, the more significant is the Auger width will be for the correspondent channel.

For $1s2s^22p$, the $1s$ electron is a spectator. Let us assume this $1s$ is spin-down. If we consider the spin configurations, strong interactions between the two $2s$ electrons and between the $2s$ spin-down electron and $2p$ spin-up electron are most probable. But, owing to the existence of a $1s$ spin-down electron, the $2s$ electron in the $2s$-$2p$ interaction cannot fall into the vacant-$1s$ shell without a spin flip. Therefore, only the Auger decay from the $2s$-$2s$ interaction is most important, which leaves the residue target system in a $1s^22p$ state.

From the resonance of $1s2s^23p$ in Table III, the ratio of the decay of $1s2s^23p$ to ground-state ion $1s^22s$ is extremely small, and this is similar to the case of $1s2s^22p$. But why is there a large portion decaying to $1s^24p$? In $1s2s^2np$ with $n>2$, the nuclear charge seen by the np orbital is screened by three inner electrons prior to the decaying process. Hence, $Z_{eff}=1$ for this np. After the Auger decay and in the $1s^2np$ channel the new np electron sees a nucleus that is only screened by two $1s$ electrons, i.e., $Z_{eff}=2$. Due to the stronger attraction of the nuclear force, the new np orbital in $1s^2np$ should be closer to the nucleus than the np in $1s2s^2np$. For this reason, the $4p$ orbital in the $1s^24p$ could have significant overlap with the $3p$ in $1s2s^23p$. Even so, the $3p$ in $1s2s^23p$ still has more overlap to the $3p$ in $1s^23p$ than that of the $4p$ orbital. The width from $1s^23p$ is larger than that from $1s^24p$. The branching ratio of $3p$:$4p$ is calculated to be 100:27, which is close to the intensity ratio 100:32 observed in the experiment [1]. For $1s2s^22p$, the p electron has the same principle quantum number as the two $2s$ electrons, and this argument does not apply.

The results of $1s2s^2np(n=4-6)$ are similar to those of $1s2s^23p$ except that the screening and effective nuclear charge effect become more pronounced. For $1s2s^24p$ decay

TABLE III. Relative intensities of the Auger decay channels of beryllium.

Resonance	Channel	PW	Relative Intensities				Auger Energy (eV)		
	$1s^2nl$	(meV)	This work	Expt. [a]	Expt. [b]	Theory [a]	This work	Chung [c]	Expt. [d]
$1s2s^22p\ ^1P^o$	$1s^22s$	0.35	1.02	1.67(11)	1.8(1)		106.186	106.20	106.0±0.2
	$1s^22p$	34.89	100.00	100	100.0	100.00	102.231	102.24	102.12±0.1
	$1s^23p$	0.23	0.66	3.49(16)	2.86(7)	0.10	94.221		
	$1s^24p$	0.02	0.06	0.71(6)	0.47(7)	0.05	91.435		
	$1s^25p$	0.00	0.01	0.29(5)	0.16(4)	0.03	90.173		
$1s2s^23p\ ^1P^o$	$1s^22s$	0.12	0.30	2.6(3)	0.01		112.093		
	$1s^22p$	0.24	0.60				108.138		
	$1s^23p$	39.74	100.00	100	100	100	108.138		
	$1s^24p$	10.73	27.01	32(1)	28.2	26.8	97.342		
	$1s^25p$	0.05	0.13		0.01		96.081		
$1s2s^24p\ ^1P^o$	$1s^22p$	0.11	0.39				109.256		
	$1s^23p$	3.83	13.37	10.8(7)		15.3	101.245		
	$1s^24p$	18.61	65.03	57(2)		61.2	98.459		
	$1s^25p$	28.62	100.00	100		100.0	97.198		
	$1s^26p$	0.47	1.64	4.3(5)		2.2	96.497		
$1s2s^25p\ ^1P^o$	$1s^22p$	0.04	0.11				109.710		
	$1s^23p$	1.26	3.34	2.3(3)		3.7	101.700		
	$1s^24p$	5.86	15.48	14(1)		14.9	98.914		
	$1s^25p$	1.74	4.60	7.2(8)		5.1	97.653		
	$1s^26p$	37.86	100.00	100		100.0	96.952		
	$1s^27p$	5.16	13.63	21(1)		15.3	96.511		
$1s2s^26p\ ^1P^o$	$1s^22p$	0.01	0.042				109.937		
	$1s^23p$	0.61	2.29			2.20	101.927		
	$1s^24p$	2.58	9.75	8.7(8)		8.60	99.141		
	$1s^25p$	1.92	7.25	15(1)		6.70	97.880		
	$1s^26p$	1.73	6.55	16(1)		4.40	97.179		
	$1s^27p$	26.44	100.00	100		100.00	96.738		
	$1s^28p$	14.52	54.92	95(4)		59.80	96.431		

[a]Jiménez-Mier *et al.* [7].
[b]Caldwell *et al.* [1].
[c]Theoretical results of Chung [10].
[d]Experimental results of Rødbro *et al.* [24].

channels, the $4p$:$5p$ ratio is less than 1, implying that the $5p$ in $1s^25p$ has a larger overlap to the $4p$ orbital in $1s2s^24p$ than the $4p$ of $1s^24p$. Similarly in $1s2s^25p$, the partial width of the $1s^26p$ channel is the largest, whereas in $1s2s^26p$, $1s^27p$ channel has the largest partial width. It is interesting to note that the the partial width of the $1s^25p$ channel is even smaller than that of the $1s^24p$ in $1s2s^25p$, but this result is supported by the experiment as well as the earlier theoretical calculation [7].

As Z increases, the total width of the four-electron resonances increases slightly. There are also changes in the Auger decay branching ratios. For larger Z, the effect of changing from Z_{eff} to $Z_{eff}-1$ becomes less important. For the decay modes of $1s2s^23p$, the Auger decay branching ratios of the $1s^24p$ channel vs that of the $1s^23p$ decreases as Z increases. This ratio of $3p$:$4p$ for Be is calculated to be 78:21, and that of F is 96:1.

For $1s2p^3$, Auger decay arises from the interaction of two $2p$ electrons. One falls into the $1s$ shell while the other escapes. This Auger decay needs an angular momentum exchange to leave the residue target system in a $1s^22p$ state. Therefore, the Auger width of $1s2p^3$ is smaller than that of $1s2s^2np$. The latter decays without an angular momentum exchange.

From C to Ne, the $1s^22p$ channel from decay of $1s2p^3$ is near 100%. Only in B, is there a significant portion decaying to $1s^23p$. This is because the energies of B $1s2p^3$ and $1s2s^23p$ are close together and the two states are nearly degenerate. The resonance is a mixture of these two configurations. Since the decay mode from $1s2s^23p$ is known to be dominated by the $1s^23p$ channel, the partial width of the $1s^23p$ channel should be significant. The ratio of $2p$:$3p$ is calculated to be 84:15. In our calculation, we find that there are 83% $sppp$ waves and 13% $sssp$ waves in B $1s2p^3$.

C. Identification of Auger spectra

The B spectrum of Rødbro *et al.* [24] was recalibrated by Chung and Bruch [25]. The identification of lithiumlike resonances in the high-resolution Auger spectra of Be and B was

TABLE IV. Auger branching ratio for berylliumlike ions.

Resonance		Auger branching ratio (%)						
	Decay channel	Be	B	C	N	O	F	Ne
$1s2s^22p\ ^1P^o$	$1s^22s+kp$	0.98	0.34	0.06	0.00	0.02	0.08	0.13
	$1s^22p+ks$	93.32	93.64	93.72	93.81	93.90	93.84	93.95
	$1s^22p+kd$	4.99	5.76	6.07	6.10	6.03	6.04	5.89
$1s2s^23p\ ^1P^o$	$1s^23p+ks$	78.09		94.61	95.68	96.08	96.26	96.29
	$1s^24p+ks$	21.09		3.10	1.79	1.17	0.84	0.64
$1s2p^3\ ^1P^o$	$1s^22s+kp$		0.04	0.01	0.02	0.03	0.03	0.03
	$1s^23s+kp$		0.27	0.01	0.00	0.00	0.00	0.00
	$1s^22p+ks$		15.03	13.49	13.23	13.03	13.09	12.65
	$1s^22p+kd$		69.28	85.22	85.92	86.34	86.44	86.93
	$1s^23p+ks$		13.32	0.16	0.08	0.06	0.04	0.08
	$1s^23p+kd$		1.59	0.97	0.66	0.46	0.34	0.27
	$1s^24p+ks$		0.30	0.02	0.01	0.01	0.01	0.00
	$1s^24p+kd$		0.17	0.12	0.07	0.06	0.04	0.03

made by Chung [10]. Energies of the $1s2s^22p\ ^1P^o$ states of Be-like ions and comparison with experimental energies in the $(1s^22s\ ^2S,e)$ and $(1s^22p\ ^2P,e)$ channels have also been carried out [4]. However, the shift from the interaction between the open- and closed-channel components was not included in these earlier works. In this work, we have included the open-channel interaction as well as adopted a larger basis set and further saturated the functional space with the restricted-variation calculation. The improved accuracy and the calculated branching ratios can be used for a more critical comparison with the observed Auger spectra.

The calculated Be $1s2s^22p\ ^1P^o\rightarrow\ (1s^22p,e)$ is at 102.23 eV. It is close to the very weak line observed at 102.12 ± 0.1 eV [24]. The corresponding $1s2s^22p\ ^1P^o\ \rightarrow\ (1s^22s,e)$ Auger energy is 106.19 eV, which is close to an even weaker line at 106.0 ± 0.2 eV. However, Chung [10] pointed out that the $1s2s2p2p\ ^5P\rightarrow\ (1s^22p,e)$ is also at 106.16 eV. Judging from the weakness of the 102.12 ± 0.1 eV line and the branch ratios calculated in this work, it is highly likely that the 106.0 ± 0.2 eV line may have come from the ^5P state rather than from this $^1P^o$. This conclusion is also consistent with the Auger spectra observed for higher-Z systems. For example, the corresponding line for the $^1P^o\rightarrow\ (1s^22s,e)$ channel is completely absent in the B spectrum of Rødbro *et al.* [24] and the C spectrum of Bruch *et al.* [26] and Mann [27], consistent with our calculated branching ratios. Since the observed lines corresponding to $^1P^o\rightarrow\ (1s^22p,e)$ are weak in the experiments, the decaying to $(1s^22s,e)$ would be invisible.

For oxygen, the $1s2s^22p\ ^1P^o$ Auger transition is studied in the experiment of Bruch *et al.* [28]. The $(1s^22s,e)$ channel intensity is very weak, in accord with the theoretical results. The intensity ratio of $(1s^22p,e)$:$(1s^22s,e)$ was found to be 16 ± 10, which is in close agreement with the theoretical result 14.7 of Nicolaides and Mercouris [29] and differs by a factor of 5 to the theoretical result 74.1 of Chen [23]. Our result is closer to the result of Chen and does not lie within the experimental uncertainty. The discrepancy between the theoretical calculations for the ratio of $(1s^22p,e)$:$(1s^22s,e)$ is not surprising. The decay rate of the $1s^22s$ channel is extremely small indicating that large cancellation exists in the matrix elements. A slight difference in the wave function may cause a small difference in the absolute value of partial width but very significant difference in this ratio. Experimentally, we note that this $(1s^22s,e)$ decay line lies on the shoulder of a very intense spectral line [28]. Any small contribution from the stronger line may cause an overestimate of decay rate for the $1s^22s$ channel. Removing this contribution will significantly increase the ratio in question.

D. Photoionization from Be $1s^22s^2\ ^1S$

In Fig. 1, we show the photoionization cross section in the nonresonant region from Be $1s^22s^2\ ^1S$. There are two open channels in this photoionization process. We have made cross-section calculation by including one channel at a time and compare the results to those with both channels included. These results are presented. It is apparent that there are cancellations in the total cross-section calculation. The value of the largest cross section in this region is about 1.4 Mb, 400 times smaller than the first peak in the resonant region in Fig. 2.

In Fig. 2, we give the resonant region for Be. The first peak in this region comes from $1s2s^22p\ ^1P^o$ resonance and is at about 530 Mb. The resonant photo energy is 155.5 eV. The second peak comes from the $1s2s^23p\ ^1P^o$ resonance. The resonant photo energy is 121.4 eV. The peak is at about 47 Mb, 10 times smaller than the first peak.

IV. CONCLUSION

In this work, we have computed the energy and width of the singly core-excited berylliumlike $^1P^o$ resonances with the saddle-point complex-rotation method for $Z=4-10$. We find that the Auger decay modes of the $1s2s^22p\ ^1P^o$ reso-

TABLE V. Auger width, branching ratio, and Auger energy for berylliumlike ions.

Resonance	Decay channels	PW (meV)	Branching ratio(%)	Auger energy (eV) This work	Chung	Experiment	Chen [a]
$B^+ 1s2s^22p\ ^1P^o$	$1s^22s$	0.15	0.34	169.326	169.35 [b]		
	$1s^23s$	0.00	0.00	146.963			
	$1s^22p$	45.13	99.40	163.332	163.34 [b]	163.38 [c]	
	$1s^23p$	0.11	0.24	145.400			
	$1s^24p$	0.01	0.03	139.190			
$B^+ 1s2p^3\ ^1P^o$	$1s^22s$	0.01	0.04	184.739	185.61 [a]		
	$1s^23s$	0.07	0.27	162.376			
	$1s^22p$	22.88	84.31	178.745	179.60 [a]		
	$1s^23p$	4.04	14.91	160.814			
	$1s^24p$	0.13	0.47	154.603			
$C^{2+} 1s2s^22p\ ^1P^o$	$1s^22s$	0.03	0.06	246.088	246.13 [d]		246.63
	$1s^23s$	0.00	0.00	208.517			
	$1s^22p$	52.60	99.79	238.089	238.11 [d]	238.0±0.2 [e] 238.21±0.2 [f]	238.54
	$1s^23p$	0.07	0.13	206.402			
	$1s^24p$	0.01	0.01	195.432			
$C^{2+} 1s2p^3\ ^1P^o$	$1s^22s$	0.00	0.01	266.809	266.88 [d]		
	$1s^23s$	0.00	0.01	229.238			
	$1s^22p$	34.62	98.71	258.809	258.87 [d]	258.56±0.2 [e] 258.6±0.2 [f]	260.58
	$1s^23p$	0.40	1.13	227.123			
	$1s^24p$	0.05	0.24	216.153			
$C^{2+} 1s2s^23p\ ^1P^o$	$1s^22s$	0.17	0.26	275.051			
	$1s^23s$	0.41	0.64	237.480			
	$1s^22p$	0.88	1.37	267.051			
	$1s^23p$	61.23	94.63	235.365			
	$1s^24p$	2.01	3.10	224.395			
$N^{3+} 1s2s^22p\ ^1P^o$	$1s^22s$	0.00	0.00	336.497			337.08
	$1s^23s$	0.00	0.00	279.920			
	$1s^22p$	57.96	99.91	326.503			326.99
	$1s^23p$	0.04	0.07	277.252			
	$1s^24p$	0.01	0.01	260.194			
$N^{3+} 1s2p^3\ ^1P^o$	$1s^22s$	0.01	0.02	362.456			
	$1s^23s$	0.00	0.00	305.879			
	$1s^22p$	42.77	99.15	352.462			354.28
	$1s^23p$	0.32	0.74	303.211			
	$1s^24p$	0.04	0.08	286.153			
$N^{3+} 1s2s^23p\ ^1P^o$	$1s^22s$	0.19	0.28	382.558			
	$1s^23s$	0.54	0.78	325.981			
	$1s^22p$	1.00	1.45	372.563			
	$1s^23p$	65.91	95.70	323.313			
	$1s^24p$	1.23	1.79	306.254			
$O^{4+} 1s2s^22p\ ^1P^o$	$1s^22s$	0.01	0.02	440.550	440.60 [g]	440.5±0.2 [h]	441.16
	$1s^23s$	0.00	0.00	361.169			
	$1s^22p$	61.90	99.93	428.559	428.59 [g]	428.5±0.2 [h]	429.07
	$1s^23p$	0.03	0.05	357.944			
	$1s^24p$	0.00	0.00	333.471			
$O^{4+} 1s2p^3\ ^1P^o$	$1s^22s$	0.02	0.03	471.799	471.89 [g]		
	$1s^23s$	0.00	0.00	392.418			
	$1s^22p$	49.57	99.37	459.807	459.88 [g]		461.63
	$1s^23p$	0.26	0.52	389.193			
	$1s^24p$	0.04	0.07	364.719			

TABLE V. (*Continued*).

Resonance	Decay channels	PW (meV)	Branching ratio(%)	Auger energy (eV) This work	Chung	Experiment	Chen [b]
O^{4+} $1s2s^23p\ ^1P^o$	$1s^22s$	0.18	0.25	507.537			
	$1s^23s$	0.72	0.99	428.156			
	$1s^22p$	1.07	1.49	495.546			
	$1s^23p$	69.55	96.10	424.932			
	$1s^24p$	0.85	1.17	400.458			
F^{4+} $1s2s^22p\ ^1P^o$	$1s^22s$	0.05	0.08	558.288			558.9
	$1s^23s$	0.00	0.00	452.301			
	$1s^22p$	65.11	99.88	544.287			544.8
	$1s^23p$	0.02	0.04	448.515			
	$1s^24p$	0.00	0.00	415.299			
F^{5+} $1s2p^3\ ^1P^o$	$1s^22s$	0.02	0.03	594.821			
	$1s^23s$	0.00	0.00	488.834			
	$1s^22p$	55.28	99.53	580.820			582.65
	$1s^23p$	0.21	0.38	485.048			
	$1s^24p$	0.02	0.05	451.832			
F^{5+} $1s2s^23p\ ^1P^o$	$1s^22s$	0.20	0.26	649.961			
	$1s^23s$	0.80	1.07	543.973			
	$1s^22p$	1.15	1.53	635.960			
	$1s^23p$	72.21	96.29	540.187			
	$1s^24p$	0.63	0.84	506.972			
Ne^{6+} $1s2s^22p\ ^1P^o$	$1s^22s$	0.09	0.13	689.739		690.6 ± 0.3 [i]	690.31 [j] 689.29 [k]
	$1s^23s$	0.00	0.00	553.338			
	$1s^22p$	68.48	99.84	673.709		673.4 ± 0.1 [l] 673.8 ± 0.1 [i]	673.17 [j]
	$1s^23p$	0.02	0.03	548.983			
	$1s^24p$	0.00	0.00	505.699			
Ne^{6+} $1s2p^3\ ^1P^o$	$1s^22s$	0.02	0.03	731.587			
	$1s^23s$	0.00	0.00	595.186			
	$1s^22p$	59.59	99.58	715.558			
	$1s^23p$	0.21	0.35	590.832			
	$1s^24p$	0.02	0.03	547.548			
Ne^{6+} $1s2s^23p\ ^1P^o$	$1s^22s$	0.21	0.27	809.662			
	$1s^23s$	0.90	1.16	673.261			
	$1s^22p$	1.22	1.56	793.633			
	$1s^23p$	74.95	96.32	668.907			
	$1s^24p$	0.50	0.64	625.623			
	$1s^25p$	0.03	0.04	605.680			

[a]Theoretical results of Chen [23].
[b]Theoretical results of Chung [10].
[c]Experimental results of Rødbro *et al.* [24].
[d]Theoretical results of Chung [11].
[e]Experimental results of Mann [27].
[f]Experimental results of Bruch *et al.* [26].
[g]Theoretical results of Chung [12].
[h]Experimental results of Bruch *et al.* [28].
[i]Experimental results of Itoh *et al.* [31].
[j]Multiconfiguration Dirac-Fock calculations in Bruch *et al.* [30].
[k]1/Z expansion in Bruch *et al.* [30].
[l]Experimental results of Bruch *et al.* [30].

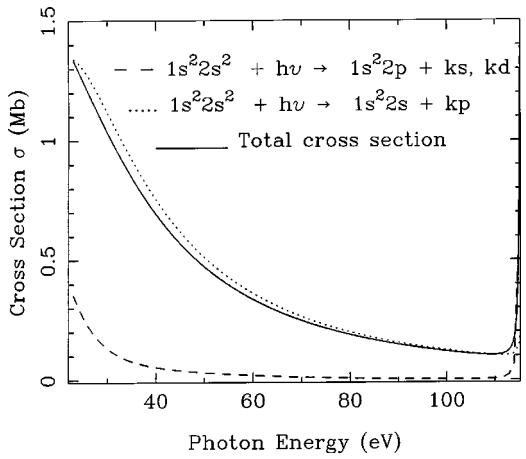

FIG. 1. The photoionization cross section from the Be $1s^2 2s^2\ ^1S$ in nonresonant region.

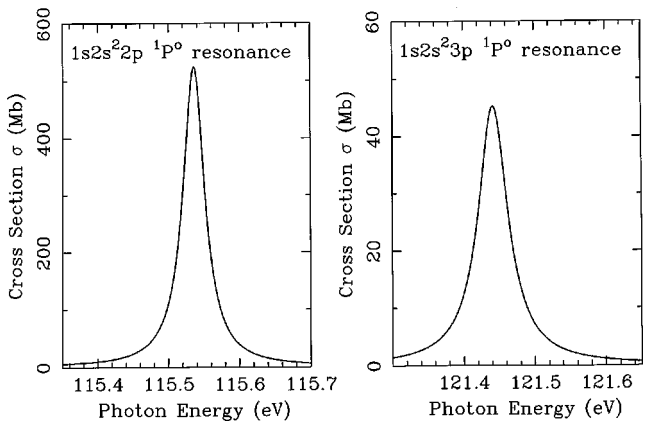

FIG. 2. Photoionization cross section for the resonance Be $1s2s^2 2p\ ^1P^o$ and $1s2s^2 3p\ ^1P^o$.

nances are very similar for different values of *Z*. This agrees with the experimental results of Caldwell *et al.* [1] and others. It confirms the conclusion that the near 100% production of the $(1s^2 2p, e)$ decay channel of $1s2s^2 2p\ ^1P^o$ is a common feature of the Be-like series [4]. Furthermore, our results about the decay modes of higher resonances of Be are also in agreement with those of Jiménez-Mier *et al.* [7], and they are good examples to support the spin-alignment-dependent theory proposed by Chung [8]. Some of the theoretical results in this work have no experimental data in the literature to compare with at present. We hope our results would be useful in more extensive studies of the Auger spectrum and photoionization spectrum of four-electron system in future experiments.

ACKNOWLEDGMENTS

This work was supported by the National Science Foundation, Grant No. PHY00-70431, and by the National Science Council of the Republic of China (Taiwan), Grant No. NSC 89-2112-M-007-062.

[1] C. D. Caldwell, M. G. Flemming, M. O. Krause, P. van der Meulen, C. Pan, and A. F. Starace, Phys. Rev. A **41**, 542 (1990).
[2] K. T. Chung, Phys. Rev. Lett. **78**, 1416 (1997).
[3] O. Grizzi and R. A. Baragiola, Phys. Rev. A **30**, 2297 (1984).
[4] K. T. Chung, Phys. Rev. A **42**, 5732 (1990).
[5] T. W. Gorczyca, Phys. Rev. A **61**, 024702 (2000).
[6] H.-L. Zhou, S. T. Manson, L. VoKy, N. Feautrier, and A. Hibbert, Phys. Rev. Lett. **87**, 023001 (2001).
[7] J. Jiménez-Mier, S. Schaphorst, C. D. Caldwell, and M. O. Krause, J. Phys. B **32**, 4301 (1999).
[8] K. T. Chung, Phys. Rev. A **59**, 2065 (1999).
[9] K. T. Chung, Phys. Rev. A **20**, 1743 (1979).
[10] K. T. Chung, J. Phys. B **23**, 2929 (1990).
[11] K. T. Chung, Phys. Scr. **42**, 530 (1990).
[12] K. T. Chung, Phys. Scr. **42**, 537 (1990).
[13] K. T. Chung, Phys. Rev. A **42**, 645 (1990).
[14] K. T. Chung, Chin. J. Phys. (Taipei) **27**, 507 (1989).
[15] S. H. Lin, C.-S. Hsue, and K. T. Chung, Phys. Rev. A **64**, 012709 (2001).
[16] W. C. Shiu, C.-S. Hsue, and K. T. Chung, Phys. Rev. A **64**, 022714 (2001).
[17] K. T. Chung and B. F. Davis, Phys. Rev. A **26**, 3278 (1982).
[18] K. T. Chung, Phys. Rev. A **56**, R3330 (1997).
[19] T. N. Rescigno and V. McKoy, Phys. Rev. A **12**, 522 (1975).
[20] K. T. Chung and X.-W. Zhu, Phys. Scr. **48**, 292 (1993).
[21] K. Berrington, J. Pelan, and L. Quigley, J. Phys. B **30**, 4973 (1997).
[22] L. Voky, H. E. Saraph, W. Eissner, Z. W. Liu, and H. P. Kelly, Phys. Rev. A **46**, 3945 (1992).
[23] M. H. Chen, Phys. Rev. A **31**, 1449 (1985).
[24] M. Rødbro, R. Bruch, and P. Bisgaard, J. Phys. B **12**, 2413 (1979).
[25] K. T. Chung and R. Bruch, Phys. Rev. A **28**, 1418 (1983).
[26] R. Bruch, K. T. Chung, W. L. Luken, and J. C. Culberson, Phys. Rev. A **31**, 310 (1985).
[27] R. Mann, Phys. Rev. A **35**, 4988 (1987).
[28] R. Bruch, S. Datz, P. D. Miller, P. L. Pepmiller, H. F. Krause, J. K. Swenson, and N. Stolterfoht, Phys. Rev. A **36**, 394 (1987).
[29] C. A. Nicolaides and T. Mercouris, Phys. Rev. A **36**, 390 (1987).
[30] R. Bruch, D. Schneider, M. H. Chen, K. T. Chung, and B. F. Davis, Phys. Rev. A **44**, 5659 (1991).
[31] A. Itoh, D. Schneider, T. Schneider, T. J. M. Zouros, G. Nolte, G. Schiwietz, W. Zeitz, and N. Stolterfoht, Phys. Rev. A **31**, 684 (1985).